Bioorganic & Medicinal Chemistry 18 (2010) 4032–4041

Contents lists available at ScienceDirect

Bioorganic & Medicinal Chemistry

journal homepage: www.elsevier.com/locate/bmc

Structural determinants for the inhibitory ligands of orotidine-5′-monophosphate decarboxylase

Maria Elena Meza-Avina [a,f], Lianhu Wei [a], Yan Liu [d], Ewa Poduch [a], Angelica M. Bello [a], Ram K. Mishra [a], Emil F. Pai [a,c,d,*], Lakshmi P. Kotra [a,b,e,f,*]

[a] Center for Molecular Design and Preformulations and Division of Cell & Molecular Biology, Toronto General Research Institute/University Health Network, Toronto, ON, Canada M5G 1L7
[b] Departments of Pharmaceutical Sciences and Chemistry, University of Toronto, Canada
[c] Division of Cancer Genomics and Proteomics, Ontario Cancer Institute/University Health Network, Toronto, ON, Canada M5G 1L7
[d] Departments of Biochemistry, Medical Biophysics, and Molecular Genetics, University of Toronto, Toronto, ON, Canada M5S 1A8
[e] McLaughlin Center for Molecular Medicine, University of Toronto, Toronto, Ontario, Canada
[f] Department of Chemistry & Biochemistry, The University of North Carolina at Greensboro, Greensboro, NC 27412, USA

ARTICLE INFO

Article history:
Received 24 February 2010
Revised 4 April 2010
Accepted 6 April 2010
Available online 9 April 2010

Keywords:
De novo nucleotide synthesis
Orotidine monophosphate decarboxylase
Pharmacophore
Nucleotide inhibitors
Non-nucleotide inhibitors

ABSTRACT

In recent years, orotidine-5′-monophosphate decarboxylase (ODCase) has gained renewed attention as a drug target. As a part of continuing efforts to design novel inhibitors of ODCase, we undertook a comprehensive study of potent, structurally diverse ligands of ODCase and analyzed their structural interactions in the active site of ODCase. These ligands comprise of pyrazole or pyrimidine nucleotides including the mononucleotide derivatives of pyrazofurin, barbiturate ribonucleoside, and 5-cyanouridine, as well as, in a computational approach, 1,4-dihydropyridine-based non-nucleoside inhibitors such as nifedipine and nimodipine. All these ligands bind in the active site of ODCase exhibiting distinct interactions paving the way to design novel inhibitors against this interesting enzyme. We propose an empirical model for the ligand structure for rational modifications in new drug design and potentially new lead structures.

1. Introduction

Orotidine-5′-monophosphate decarboxylase (ODCase) catalyzes the decarboxylation of OMP (**1**) to UMP (**2**) in the de novo pathway for the transformation of the amino acid, aspartic acid to UMP. ODCase has attracted much attention from biochemists because of its status as one of the most proficient enzymes in Nature accelerating the rate of decarboxylation by over 17 orders of magnitude to produce the key pyrimidine nucleotide, UMP.[1–3] Pyrimidine nucleotides are important building blocks for the synthesis of RNA and DNA, molecules essential for cell replication and survival. Due to its important role in the de novo nucleic acid biosynthesis, ODCase is present in most species including bacteria, parasites and humans but not in viruses. Viruses depend on their host cells for the supply of nucleotides. In humans, pyrimidine nucleotides are synthesized via two routes: the de novo and salvage pathways.[4] Whenever higher concentrations of pyrimidines are needed in the cell, including for the normal cellular processes, during uncontrolled growth of the cell such as in cancer, or fast replicating viral infections etc, de novo pyrimidine synthesis is upregulated, and the activity of ODCase is simultaneously operating at a higher than normal level.[5,6]

In certain higher-level organisms, such as mouse or human, ODCase is part of the bifunctional enzyme, UMP synthase.[7] While in pathogenic organisms, such as bacteria, fungi and parasites, ODCase is a monofunctional enzyme, although in *Plasmodia* it forms a heterotetramer with orotate phosphoribosyltransferase.[8–10] In all species, ODCase seems to be active as a dimer and the catalytic site is comprised of active residues from the second monomer. *Plasmodia* such as *Plasmodium falciparum* and *Plasmodium vivax* are dependent on their own de novo synthesis of pyrimidine nucleotides due to their lack of the salvage pathway.[11] Thus, inhibition of plasmodial ODCase was proposed as a strategy for compounds directed against malaria, and a limited number of orotate analogs were investigated as potential drugs against the malaria parasite.[12–14] ODCase has also been identified as a potential target for drugs directed against RNA viruses like pox and flaviviruses.[15–18] ODCase inhibitors have

Abbreviations: ODCase, orotidine-5′-monophosphate decarboxylase; OMP, orotidine-5′-monophosphate; UMP, uridine-5′-monohosphate; BMP, barbiturate ribonucleoside-5′-monophosphate; CMP, cytidine-5′-monophosphate; XMP, Xanthosine-5′-monophosphate; *Mt*, *Methanobacterium thermoautotrophicum*; *Hs*, *Homo sapiens*; *Sc*, *Saccharomyces cerevisiae*; *Pf*, *Plasmodium falciparum*; *Hp*, *Helicobacter pylori*; *Sa*, *Staphylococcus aureus*.

* Corresponding authors. Tel.: +1 416 581 7601; fax: +1 416 581 7621 (L.P.K.).
E-mail address: lkotra@uhnres.utoronto.ca (L.P. Kotra).

0968-0896/$ - see front matter © 2010 Elsevier Ltd. All rights reserved.
doi:10.1016/j.bmc.2010.04.017

also been effective against West Nile virus, a recent thread to humans and birds in the US and Canada.[19] In the recent years, an increased interest in ODCase as a drug target is also due to the advances in determining the three-dimensional structures of this enzyme from various species. Since 2000, when the first X-ray structures of ODCase were resolved, there are now almost 100 coordinate sets of ODCase from at least 11 different species deposited in the Protein Databank (www.rcsb.org). These crystal structures were determined for the apo-form of the protein but mostly in complex with a variety of ligands such as UMP (**2**), 6-aza-UMP (**3**), BMP (**4**), XMP (**5**), CMP (**6**), as well as with a variety of mutant forms of ODCase. Despite such intense efforts in recent years, the catalytic mechanism of ODCase is still not completely understood and the use of structure-based tools in the rational design of substrate analogs of ODCase as inhibitors is still rudimentary at best.

Recently, investigations on the mechanism of decarboxylation by ODCase have gained momentum and there is compelling evidence that a C6 carbanion-based transition-state is formed during the decarboxylation.[20,21] This transition-state intermediate appears during the early stage of the reaction, and electrostatic stress may play a role in the process of decarboxylation, although other mechanisms using computational and kinetic isotope methods suggest alternatives.[20–24] We have recently revealed that under suitable conditions ODCase can facilitate interesting reactions other than decarboxylation, such as the transformation of 6-cyano-UMP (**9**) into BMP (**4**).[25,26] Based on the catalytic promiscuity exhibited by ODCase, Wittmann et al. proposed the possibility of a covalent mechanism as a unifying means of addressing various biochemical reactions undertaken by ODCase.[27] Our group has disclosed a comprehensive time-resolved crystallography and mutant analyses on the interactions and catalysis of **9** with ODCase.[26] The structural evidence in these studies compels us to believe that the slow catalysis for the transformation of **9** into **4** represents non-covalent catalysis, involving strong electrostatic forces breaking the resonance established in the 6-cyano-pyrimidine nucleic base.[26] ODCase also exhibits plasticity in accepting various nucleotide ligands including compounds such as XMP (**5**) and in fact these compounds are among the potent inhibitors of this enzyme.[28] It is also interesting to note that ODCases from various species exhibit different binding affinities towards the same inhibitors.[27] The new generation of inhibitors such as the novel C6-substituted uridine derivatives targeting ODCase specifically are exhibiting interesting and promising therapeutic activities.[29–31]

Nucleosides are well established as a major source of drugs for the treatment of cancer and viral infections.[32,33] A classic example of an unconventional nucleoside of medicinal interest, and a potent inhibitor of ODCase is pyrazofurin (also known as pyrazomycin, **7**, Fig. 1). This compound was originally isolated from the broth filtrates of *Streptomyces candidus*.[34,35] It has been the subject of numerous investigations over the past three decades due to its *C*-nucleoside status and its breadth of clinically relevant biological activities.[12] Pyrazofurin exhibits potent anticancer activity, especially against leukemia cell lines.[36–38] In clinical trials, pyrazofurin was administered to cancer patients at various doses to evaluate its potential as an anticancer agent. However, its development was abandoned later due to toxicity.[39] Pyrazofurin has also been evaluated as an antiviral agent targeting respiratory syncytial virus (RSV), influenza, vaccinia, West Nile virus and other RNA viruses.[19,40–42] Additionally, this compound has been shown to be effective against parasitic infections specifically *Plasmodium falciparum* and also was implicated in immunosuppressive therapy.[13,43] With such a long history, pyrazofurin as well as other pyrazole-based nucleosides are continuing to generate interest in medicinal chemistry.[44] The 5′-monophosphate derivative of pyrazofurin (**8**) is a potent inhibitor of *Saccharomyces cerevisiae* ODCase with inhibition constants in the low nanomolar range.[35]

Due to this exciting and rich biological activity profile at the molecular and clinical levels, our group is interested in further characterizing the interactions of pyrazofurin-5′-monophosphate (**8**) and other substrate analogs such as BMP (**4**), and 5-cyano-UMP (**10**) along with non-nucleoside inhibitors with ODCase to define pharmacophore features for substrate analogs. An empirical structural dissection and a pharmacophore model are presented based on the atomic level interactions for the potential design of novel classes of compounds targeting ODCase.

2. Experimental section

2.1. Synthesis

General. Anhydrous chemical reactions were performed under a nitrogen atmosphere. All solvents and reagents were obtained

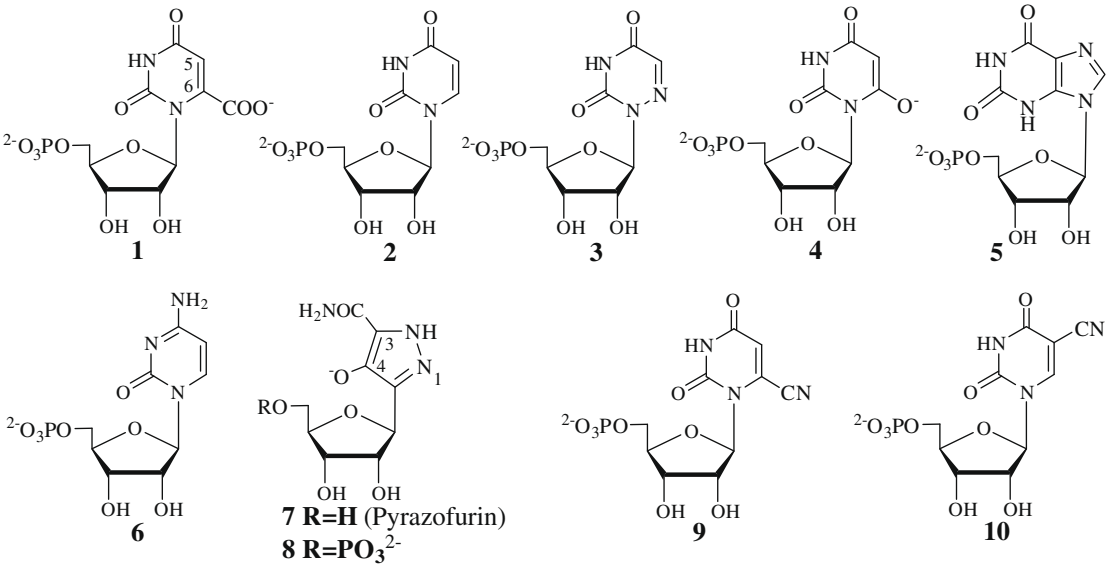

Figure 1. OMP (**1**), UMP (**2**), 6-aza-UMP (**3**), BMP (**4**), XMP (**5**), CMP (**6**), pyrazofurin (**7**), pyrazofurin-5′-monophosphate (**8**), 6-cyano-UMP and (**9**) 5-cyano-UMP (**10**).

from commercial sources. NMR spectra were recorded on a Varian spectrometer (300 or 400 MHz for ^{1}H, and 121.46 MHz for ^{31}P). Chemical shifts are reported in ppm using H_2O as the reference for the ^{1}H NMR spectra, and phosphoric acid as an external standard for the ^{31}P spectra. Mass spectra were obtained on a Q-Star mass spectrometer using ESI or EI techniques. The monophosphate derivatives were transformed into the corresponding ammonium salts by treatment with 0.5 M NH_4OH solution at 0 °C followed by lyophilization. Purity of the compounds **8** and **10** was checked on a Waters Delta 660 HPLC system attached to a PDA detector, using a Waters ODS2 5 micron reverse phase (4.6 × 100 mm) column, was >95%. The eluting system was either 100% H_2O or 95% H_2O/5% MeOH at a flow rate of 0.5 mL/min. All HPLC solvents were filtered through Waters membranes (47 mm GHP 0.45 μm, Pall Corporation) and degassed with helium. Injection samples were filtered using Waters Acrodisc® Syringe Filters 4 mm PTFE 0.2 μm.

2.1.1. 4-Hydroxy-5-(5-*O*-monophosphoryl-β-D-ribofuranos-1-yl)-1*H*-pyrazole-3-carboxamide (8)

Pyrazofurin (**7**) (11 mg, 0.042 mmol) was dissolved in triethyl phosphate (0.5 mL) and the solution was stirred at 45 °C for 10 min under a nitrogen atmosphere. The reaction mixture was cooled to 0 °C and $POCl_3$ (23.7 μL, 0.25 mmol) was added and stirring continued at the same temperature for an additional 5 h. The reaction was then quenched with cold water (1.5 mL), washed with diethyl ether (5 × 2 mL) and neutralized with 0.5 M NH_4OH. The volume of the aqueous layer was reduced under vacuum, and the crude was purified by HPLC to obtain the target compound **8**. UV λ_{max} (pH 8) 263 nm (ε = 2,477); ^{1}H NMR (D_2O) δ 4.82 (d, J = 5.9 Hz, 1H, H-1′), 4.26 (br m, 1H, H-2′), 4.13 (br m, 1H, H-3′), 4.04 (br m, 1H, H-4′) 3.93 (br m, 2H, H-5′); ^{31}P NMR (D_2O) δ 0.40 ppm; HRMS (ESI −ve) calculated for $C_9H_{13}N_3O_9P$ (M^-): 338.0394, found 338.0407.

2.1.2. 1-(5-*O*-*t*-Butyldimethylsilyl-2,3-*O*-isopropyl-β-D-ribofuranosyl)-5-cyanouracil (12)

Compound **11**[23] (2.6 g, 5.44 mmol) was dissolved in 20 mL of anhydrous DMF and treated with NaCN (0.43 g, 8.77 mmol) at 100 °C for 3 h. After this time, the reaction mixture was diluted with water (20 mL) and the pH brought to 6; the solution was extracted (3×) with 30 mL of ethyl acetate, the organic layer was washed with brine, dried with sodium sulfate, evaporated. Purification by column chromatography (hexanes/ethyl acetate, 9:1) gave **12** as a white powder (2.21 g, 96%). ^{1}H NMR ($CDCl_3$) δ 0.13 (s, 6H), 0.91 (s, 9H), 1.37 (s, 3H), 1.60 (s, 3H), 3.82 (dd, 1H, H-5′), 3.98 (dd, 1H, H-5′), 4.53 (m, 1H, H-4′), 4.69 (dd, 1H, H-2′), 4.73 (dd, 1H, H-3′), 5.89 (d, 1H, H-1′), 8.32 (s, 1H, H-6), 8.96 (broad, 1H, NH).

2.1.3. 1-β-D-Ribofuranosyl-5-cyanouracil (13)

Compound **12** (2.2 g, 5.20 mmol), was treated with 20 mL of 50% trifluoroacetic acid at 0 °C, and the reaction mixture was stirred at rt for 3 h. After this time, solvent was evaporated and the residue was purified by column chromatography (dichloromethane/methanol, 8:2) to obtain **13** as a light solid (1.3 g, 93%). UV λ_{max} = 278 nm; ^{1}H NMR (CD_3OD) δ 3.78 (dd, 1H, H-5′), 3.95 (dd, 1H, H-5′), 4.05 (m,1H, H-4′), 4.19 (m, 2H, H-2′, H-3′), 5.83 (d, 1H, H-1′), 9.02 (s, 1H, H-6); ^{13}C NMR (CD_3OD) 162.15, 151.25, 150.898, 114.76, 92.17, 90.15, 86.25, 76.47, 70.14, 61.15; HRMS (ESI) calculated for $C_{10}H_{12}N_3O_6$ (M+H) 270.0720, found 270.0725.

2.1.4. 1-(5-Monophosphoryl-β-D-ribofuranos-1-yl)-5-cyanouracil (10)

To a solution of water (0.05 mL, 2.78 mmol), CH_3CN (4.3 mL), pyridine (0.39 mL, 4.8 mmol) and $POCl_3$ (0.612 g, 0.037 mL, 4 mmol) at 0 °C, were added 0.269 g (0.702 mmol) of compound **13**. The reaction mixture was stirred for 5 h (3 h at 0 °C and then at room temperature). The reaction was monitored by TLC (*n*-butanol, water and acetic acid, 2:2:1). After the starting material was consumed, the reaction was quenched with 2 mL of cold water and stirred for an additional 2 h at rt. The solvent was evaporated and then the product was purified by passing through a basic Dowex column (eluted with water followed by 5% formic acid). The concentrated product was then dissolved in 3 mL of cold water and neutralized with NH_4OH. The solvent was evaporated and the product was lyophilized to give 0.287 g (yield 75%) of **10** as a white solid. UV λ_{max} = 278 nm (ε = 1949); ^{1}H NMR (CD_3OD) δ 4.11 (dd, 1H, H-5′), 4.22–4.27 (m, 3H, H-3′, H-4′, H-5′), 4.33 (dd, 1H, H-2′), 5.86 (d, 1H, H-1′), 8.63 (s, 1H, H-6). ^{31}P (D_2O) 0.12 (s), HRMS (ESI) calculated for $C_{10}H_{11}N_3O_9P$ (M^-) 348.0227, found 348.0238.

2.2. ODCase production

ODCases from *Methanobacterium thermoautotrophicum*, *Plasmodium falciparum* and *Homo sapiens* were cloned, expressed and purified as described previously.[23,27] Production and purification of the *Helicobacter pylori* and *Staphylococcus aureus* enzymes will be described elsewhere.[45] Enzyme concentrations were determined using a BioRAD protein assay kit with bovine serum albumin as standard.

2.3. Enzymology

Assays were performed on a VP-ITC microcalorimeter (MicroCal). For isothermal titration calorimetry (ITC) experiments, the initial delay (60 s), stirring speed (300 rpm), reference power (15 μcal/s), and the frequency of data point collection (or filter period, 1 s) were identical for all experiments. The *Hs*- and *Mt* ODCase stock solutions were prepared using 50 mM Tris (pH 7.5), 20 mM DTT, and 40 mM NaCl, and incubated overnight at rt. For injection into ITC, the substrate was dissolved in 50 mM Tris to a final concentration of 5 mM. All inhibitor solutions were prepared in the same 50 mM Tris buffer. The assay buffer for the enzyme or enzyme/inhibitor samples consisted of 50 mM Tris (pH 7.5) and 1 mM DTT, and was degassed prior to use. The activity of *Mt* ODCase (final concentration 20 nM) was determined at 55 °C. Each reaction was initiated by an 11.4 μL injection of substrate solution (5 mM). The final substrate concentration in the 1.3 mL calorimetric cell was 40 μM. The activity of *Hs* ODCase (final concentration 60 nM) was determined in the presence of 20 μM substrate at 37 °C, and the reaction was initiated by a 5.7 μL injection of substrate solution (5 mM).

Both *Mt* and *Hs* ODCases were tested against 5-fluoro-6-amido-UMP (**11**) in a reversible inhibition assay. The final concentration of *Mt* ODCase was 20 nM while the concentration of **11** was 0.5, 1, 2.5, and 5 mM. *Hs* ODCase (60 nM) was exposed to 0.1, 0.25, 0.5, and 1 mM of **11**. The volume and the final concentration of the substrate were the same as described for the controls. The concentrations of compound **8** were 5, 10, 20, and 40 μM against *Mt* ODCase. The inhibition of 60 nM *Hp* ODCase was determined using 0.25, 0.5, 1, and 1.5 μM of compound **8**.[46]

5-Cyano-UMP (**9**) was tested against *Pf*, *Hp* and *Sa* ODCases.[44] The final concentration of the *Pf* ODCase and the substrate in the reaction assay was 60 nM and 12 μM, respectively. The concentration of the inhibitor was 0.5, 1, 2, 2.5, and 5 mM. The reversible inhibition of *Hp* ODCase (60 nM) was tested in the presence of 0.25, 1, 1.5, and 2.5 mM of **10**. The reversible inhibition assay with 30 nM *Sa* ODCase was performed using the following concentrations of **10**: 0.1, 0.25, 0.5, 0.75, and 2 mM. The concentration of the substrate used in the assays with *Hp* and *Sa* ODCases was 20 μM.

Inhibition kinetics of compound **8** against *Hs* ODCase were determined using UV spectroscopy. The absorption maxima of the ligands permitted a reliable UV-based kinetics assay. *Hs* ODCase stock solution (60 μM) was prepared in 50 mM Tris (pH 7.5), 20 mM DTT, and 40 mM NaCl, and incubated overnight at room temperature. Assay samples were prepared by diluting 3 μL of the stock enzyme solution in 50 mM Tris containing 1 mM DTT to a final volume of 990 μL. Each reaction was initiated by the addition of 10 μL of the ligand (either substrate, or substrate mixed with the inhibitor). The final concentrations of *Hs* ODCase and OMP were 180 nM and 50 μM, respectively. The concentrations of compound **8** were 1, 1.5, 2, 2.5, 3, and 4 μM. After the addition of ligand, the sample was mixed quickly, and the absorption at 285 nM was recorded on a Shimadzu UV-2401PC spectrophotometer as a function of time.

The K_M values for *Hs* and *Mt* ODCases (from ITC measurements) were 1.7 ± 0.1 and 3.7 ± 0.2 μM, respectively. And the K_M for *Hs* ODCase was 3.4 ± 0.5 μM as determined by UV spectroscopy.

Data analysis: The procedure used for the determination of competitive inhibition constants was described earlier.[47] The data were fitted in Grafit 7.0 to (Eq. (1)) to calculate the K_i for each inhibitor.

$$v = \frac{V_{max}[S]}{K_M(1 + \frac{[I]}{K_i}) + [S]} \quad (1)$$

Inhibition of Hs ODCase by **8**: Compound **8** is a slow tight binding inhibitor of *Hs* ODCase. The rate of consumption of the substrate was converted into the rate of product formation using (Eq. (2)):

$$P = v_s t + \frac{v_i - v_s}{k_{obs}}[1 - \exp(-k_{obs}t)] \quad (2)$$

where v_i represents the initial rate and v_s is the steady-state rate. The parameter k_{obs} corresponds to the rate constant for the conversion from initial to steady-state rate. The initial phase of slow and reversible inhibition is represented by (Eq. (3)).

$$E \underset{k_4}{\overset{k_3[I]}{\rightleftharpoons}} EI \quad (3)$$

The relationship between [*I*] and k_{obs} is linear, and the data fit to (Eq. (4)) yields the association and dissociation constants (k_3 and k_4):

$$k_{obs} = k_3[I] + k_4 \quad (4)$$

The apparent inhibition constant K_i^{app} is calculated from the ratio of k_4/k_3. The true inhibitor dissociation constant K_i is determined by (Eq. (5)):

$$K_i^{app} = K_i\left(1 + \frac{[S]}{K_M}\right) \quad (5)$$

2.4. Crystallization and crystallographic analysis

All crystals were grown at rt using the hanging-drop method and mixing 2 μL of protein solution of 10 mg/mL enzyme in either 25 mM Tris·HCl, pH 8.0, 40 mM NaCl, 5% glycerol for complexes of *Hs* ODCase with compounds **4** and **10** or in 50 mM Tris·HCl, pH 8.5, 100 mM NaCl and 5 mM β-mercaptoethanol for compound **8**, with 2 μL of the respective reservoir solution. The best co-crystals of *Hs* ODCase with both BMP (**4**) and 5-cyano-UMP (**10**) were grown in 100 mM Tris·HCl, pH 8.4, 2.12 M ammonium sulfate while the complex with compound **8** had the best results in 100 mM Tris·HCl, pH 8.4, 1.4 M ammonium sulfate. The crystals with compounds **4** and **8** adopted space group $C222_1$ with unit cell dimensions of a = 77.6 Å, b = 116.9 Å, c = 62.0 Å and a = 79.4 Å, b = 116.5 Å, c = 62.1 Å, respectively. Crystals of the complex with compound **4** also grew in space group $C222_1$ but with unit cell axes a = 77.6 Å, b = 116.9 Å, c = 62.0 Å, whereas the complex with compound **10** grew in space group $P2_1$ with unit cell dimensions of a = 69.5 Å, b = 61.6 Å, c = 70.9 Å, β = 111.8°.

For data collection, the crystals were either transferred to reservoir solution containing 20% glycerol for cryoprotection or dipped into paratone oil before they were flash-frozen in a stream of boiling nitrogen. Diffraction data for the crystals of *Hs* ODCase co-crystallized with **4** were collected at 100 K and λ = 0.9002 Å at beam line 14BM-C, BioCARS, Advanced Photon Source, Argonne National Laboratories; data for the pyrazofurin-MP (**8**) and 5-CN-UMP (**10**) complexes were collected at 100 K and λ = 0.97949 Å and λ = 0.97934 Å, respectively, at beam line 08ID-1 of the Canadian Macromolecular Crystallography Facility, Canadian Light Source. Data were reduced and scaled using the program package HKL2000.[47] Data collection statistics are given in Table 1.

The structures of all complexes were determined using molecular replacement techniques with the help of the program package MOLREP[48] subsequent refinements were done with Refmac-5.2,[49] and model building with COOT.[50] Refinement statistics are also listed in Table 1. Atomic coordinates and structure factors have been deposited in the Protein Data Bank (PDB IDs: 3BGG, 3MI2 and 3BK0 for the complexes with ligands **4**, **8** and **10**, respectively).

2.5. Computer modeling

The three-dimensional structure of the *Hs* ODCase complex with 6-NH_2-UMP (PDB code: 3DBP) was used as the protein framework for the docking study. The ligand and the crystallographic waters were removed from the active site, and hydrogens were added to the entire protein, preparing the active site for docking. The non-nucleoside ligands, nifedipine and nimodipine were docked using Surflex-Dock, a module in the SYBYL molecular modeling package, for various docking poses and their relative ranking.

Table 1
Data collection and refinement statistics for the X-ray crystal structures of the ODCase complexes of the inhibitors, **4**, **8** and **10**

	Hs ODCase + **4**	*Hs* ODCase + **8**	*Hs* ODCase + **10**
Diffraction data			
Resolution (Å)	1.93 (1.96–1.93)	1.20 (1.30–1.20)	1.60 (1.66–1.60)
Measured reflections (n)	149,221	525,889	193,939
Unique reflections (n)	21,306	78,679	58,529
Completeness (%)	95.3 (74.6)	87.0 (60.0)	78.5 (21.7)
Rsym (%)	13.0 (50.0)	2.8 (30.6)	5.8 (32.3)
Space group	$C222_1$	$C222_1$	$P2_1$
Unit cell dimensions (Å) a	77.6	79.4	69.5
b	116.9	116.5	61.6
c	62.0	62.1	70.9
Unit cell angle (°) α, β, χ	90, 90, 90	90, 90, 90	90, 118.9, 90
Molecules in asymmetric unit (n)	1	1	2
Refinement statistics			
Resolution (Å)	50.0–1.93 (1.98–1.93)	30.4–1.20 (1.23–1.20)	50.0–1.60 (1.63–1.60)
Protein atoms (n)	2,025	2,543	4,167
Water molecules (n)	132	348	256
Reflections used for R_{free} (n)	1048 (54)	3965 (166)	2938 (49)
R_{work} (%)	18.1 (25.0)	17.2 (27.3)	17.9 (27.5)
R_{free} (%)	21.0 (25.3)	18.8 (25.1)	21.6 (33.7)
Root mean square deviation bond length (Å)	0.010	0.010	0.010
Root mean square deviation bond angle (°)	1.6	1.5	1.5
Average B-factor (Å^2)	27.1	15.9	22.4

Numbers in brackets are for the highest resolution shells. $R_{sym} = S|I - \langle I\rangle|/\sigma I$, where I is the observed intensity and $\langle I\rangle$ is the average intensity from multiple observations of symmetry-related reflections.

This process involves first, the active site was coated with three types of probes, depending on the properties of the enzyme residues exposed into the active site: CH_4 for steric, N–H for HB donor, C=O for HB acceptor. Then the ligand fragments were generated and posed into binding site to generate the best fitting pose for the ligand. The Hammerhead, a completely automatic, fast docking procedure was used to dock these two compounds to binding site. The top ranking conformation of the ligand in the binding pocket was used to analyze the interactions.

For ligand conformational analysis, eleven co-crystal structures of ODCase with eleven ligands were collected, and the inhibitors were extracted from the corresponding active sites. These structures include UMP (1DBT), 6-aza-UMP (1DVJ), 5-I-UMP (2QCH), BMP (1X1Z), 6-NH_2-UMP (2Q8Z), 5-Br-UMP (2QCG), 5-CN-UMP (3BKO), 5-F-UMP (2QCF), 6-acetyl-UMP (3L0K), 6-I-UMP (covalent complex, 3BGJ) and OMP (1KM6).

3. Results and discussion

In this study, the overarching goal is to bring together structurally diverse but potent ligands of ODCase and investigate their interactions with the active site of ODCase. As mentioned above, first we focused on three structurally diverse nucleoside ligands of ODCase. BMP (**4**), one of the ligands included in this study, carries a hydroxyl moiety at the C6 position and is the most potent inhibitor of ODCase with a K_i of 8.8×10^{-12} M for the yeast enzyme.[51] Both the C6 hydroxyl moiety in **4** and the C4 substitution in **8** are similar in their location and their ability to present the anionic moiety for transition-state mimicry. Pyrazofurin-5′-monophosphate (**8**) is a *C*-nucleoside carrying a pyrazole moiety instead of the pyrimidine nucleic base, and does not possess the typical glycosidic bond similar to the natural *N*-nucleoside. In fact pyrazofurin (**7**) was one of the very few *C*-nucleosides evaluated clinically as an anticancer and antiviral agent.[12] The corresponding mononucleotide **8** binds tightly at the active site of ODCase, thus this compound was of great interest to us and we investigated its interactions with the protein matrix in greater detail. Structurally, the presence of cyano substituent at the C5 position of compound **10** was not only intended to provide clues on the interactions of the 5-CN moiety with ODCase, but also test whether any unusual chemistry could be observed as had been the case with 6-CN-UMP.[23,24]

Compound **4** was synthesized according to the reported procedure.[52] The mononucleotide derivatives of **8**, and **10** were synthesized according to Scheme 1. Compound **10** was synthesized from the fully protected 5-bromouracil derivative **11** by treatment with sodium cyanide to obtain compound **12** followed by deprotection with aqueous TFA to give **13** (Scheme 1A). 5-Cyanouridine (**13**) was phosphorylated by treatment with $POCl_3$ to yield **10**. Pyrazofurin (**7**) was phosphorylated using triethyl phosphate and $POCl_3$ to obtain compound **8** (Scheme 1B). For enzymatic studies, *Hs*, *Mt*, *Sa*, *Pf* and *Hp* ODCase, that is, enzymes from species spanning higher organisms, *Archaea* and bacteria were employed. Compounds **4**, **8** and **10** were co-crystallized with *Hs* ODCase and the corresponding three-dimensional structures were determined to detail the atomic interactions in the binding site of *Hs* ODCase (1.93, 1.2 and 1.6 Å resolution, respectively, Fig. 2).

The active site architectures for the ODCase complexes with **4**, **8** and **10** are almost identical, and there are no major differences in the conformations of the residues that comprise the active site. An analysis of the hydrogen-bonding network, however, allows one to identify the similarities and differences for the different ligands (Fig. 3). The phosphoribosyl moiety in all three inhibitors exhibited very similar interactions with the enzyme. This portion of the nucleotide engages in a network of hydrogen-bonding interactions, primarily through the 2′ and 3′ hydroxyl moieties as well as the phosphoryl moiety at the 5′-position. This is a typical feature found in the other inhibitor complexes of ODCase and this interaction is responsible for a large contribution towards the binding energy.[53,54]

In the active site of ODCase, BMP (**4**) positions its highly acidic hydroxyl moiety at C6 close to the side chains of Lys125 and Asp123, which are both part of a strong network of ionic bonding interactions (Fig. 2E,F, and Fig. 3C). Close by, the presence of a tightly bound water molecule (2.75 Å distance from 6-OH moiety) correlates well with BMP binding, probably mitigating the potency of BMP to interact with ODCase (Fig. 3C). 5-Cyano-UMP on the other hand does not carry any C6 substitution but a neutral cyano group at the C5 position that fits well into a small hydrophobic pocket in the active site. The remaining parts of the respective nucleic base of **4** and **10** interact with the ODCase active site in very similar fashion, mostly through conserved hydrogen bonds. For example, the O2, N3 and O4 atoms in **4** and **10** exhibit almost identical interactions with the side chains of Gln241, Ser183 and a crystallographic water molecule (Fig. 3B and C). At physiological pH, the hydroxyl moiety is deprotonated and presents compound **4** as a transition-state analog, a feature described earlier.[3,20,21]

The *C*-Nucleoside analog pyrazofurin (**7**) and its monophosphate derivative **8** are pharmacologically well-characterized compounds. Little is known, however, of **8**'s interactions with its target enzyme ODCase. Pyrazofurin does not have the typical glycosidic bond present in *N*-nucleosides (Fig. 4). The pyrazole moiety is attached via the C5 carbon to the C1′ position of the ribosyl moiety, and in addition, carries two key substitutions on the pyrazole moiety: an amido moiety at C3 and a hydroxyl moiety at C4 position (Fig. 4). This hydroxyl moiety (pK_a 6.7) would be deprotonated

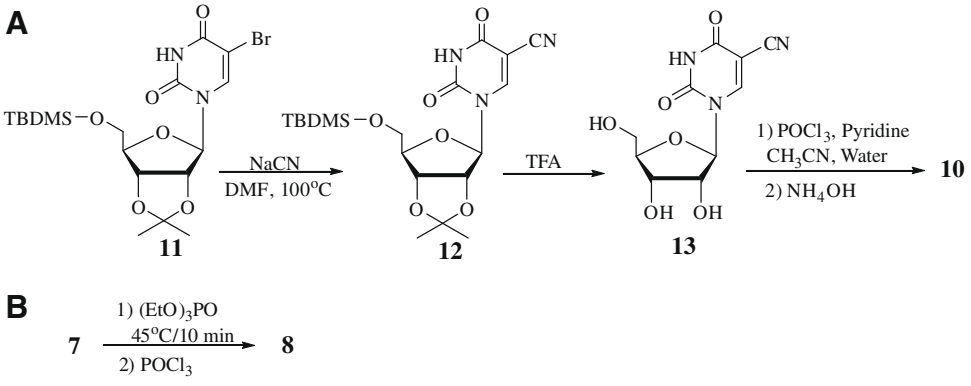

Scheme 1. Synthesis of compound **8** and **10**.

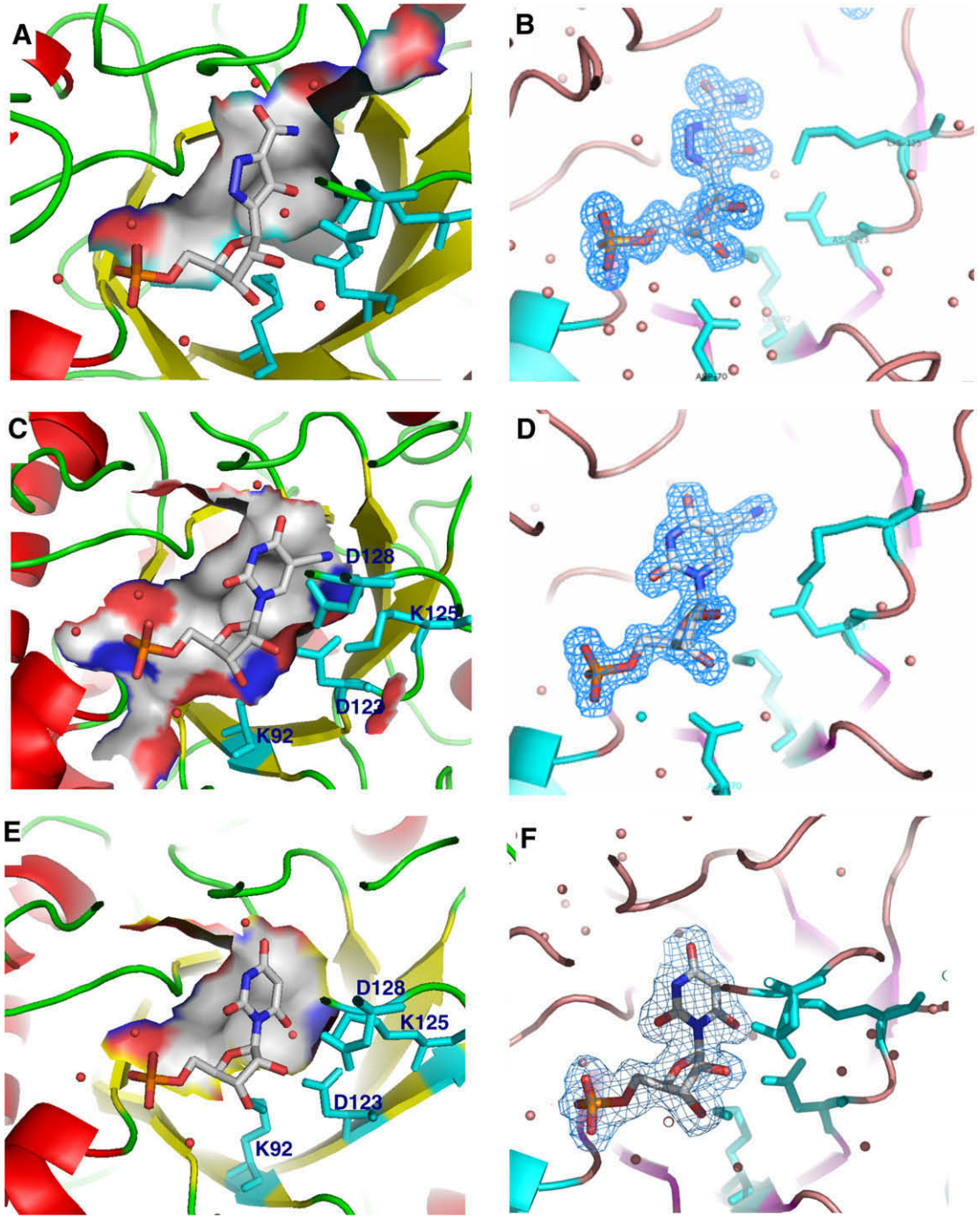

Figure 2. The active sites of ODCase as seen in the co-crystal structures of the complexes of **8** (panels A and B), **10** (panels C and D), and **4** (panels E and F) with *Hs* ODCase. Panels B, D and F depict the electron densities ($2F_o - F_c$) corresponding to the inhibitor molecules, displayed at 1σ level. Enzyme backbones are rendered according to their secondary structures, and the ligands are shown in capped-stick representation.

to a large extent at physiological pH (7.4), similar to what is found with BMP (**4**). It is anticipated that the hydroxyl moiety could mimic the transition-state species, again similar to BMP, when bound to the active site of ODCase. Thus we co-crystallized pyrazofurin-5′-monophosphate (**8**) with *Hs* ODCase and determined the three-dimensional structure of the complex at 1.2 Å resolution (Table 1, Fig. 2A,B, and Fig. 3A). The aza-moiety in the pyrazole ring of **8** interacts via hydrogen bonds with the side chains of Gln241 and Ser183 (Fig. 3A). These hydrogen bonds account for the interactions of O2 and N3 in a typical pyrimidine nucleic base (Fig. 3A vs C). The carbonyl moiety in the C3 amido group of the pyrazole ring interacts with the backbone nitrogen of Ser183 and a water molecule, equivalent to the interactions of the O4 moiety in the natural uracil ring. This pattern of strong interactions locks the orientation of the pyrazole moiety in the ODCase binding site presenting other functional groups to the conserved catalytic residues (Fig. 2A).

The second set of interactions of the pyrazole moiety includes the salt bridge between the ionized hydroxyl group linked to C4 and the positively charged side chain of Lys125 as well as two hydrogen bonds with bound water molecules (d = 2.6–2.9 Å). Although these interactions of the pyrazole moiety in **8** are not identical to those seen with the pyrimidine nucleic base in **4**,

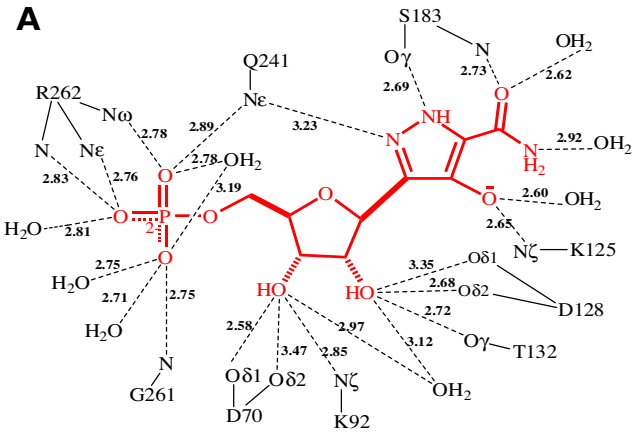

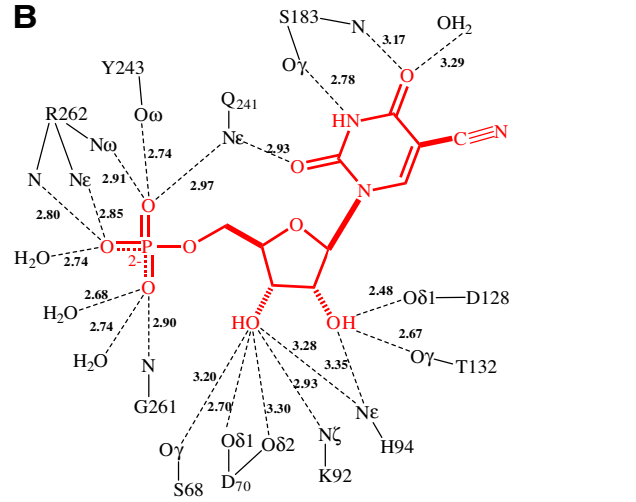

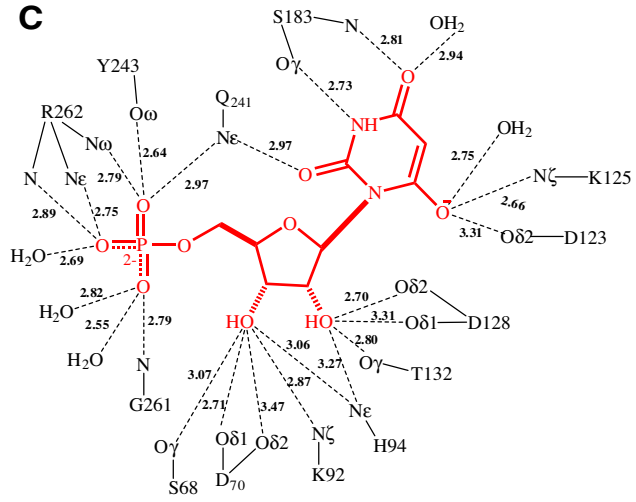

Figure 3. Schematic of the interactions of **8**, **10** and **4** with the active site of *Hs* ODCase (panels A, B and C, respectively).

equivalent electrostatic and steric interactions nevertheless result in tight binding of **8** to ODCase (Fig. 3A vs C). Our results assert that the heterocycle on the ribose can be varied without compromising binding affinity; in this particular case, pyrimidine and pyrazole provided the same 'backbone' environment to the ligand structure. Purine heterocycles can also be substituted, as recently reported for xanthosine-5′-monophosphate (**5**, Fig. 1), another highly potent inhibitor of ODCase.[27] Even molecules like nifedipine and nimodipine (**14** and **15**, respectively, Fig. 4), clinically used calcium channel blockers, inhibit ODCase competitively, with inhibition constants (K_i) of 105 and 18 μM, respectively.[55] These observations contribute to the mounting evidence that ODCase, although evolved to carry out the decarboxylation of OMP with high efficiency, is inherently promiscuous in binding to other nucleosides, both purines and pyrimidines, as well as to non-nucleoside inhibitors.

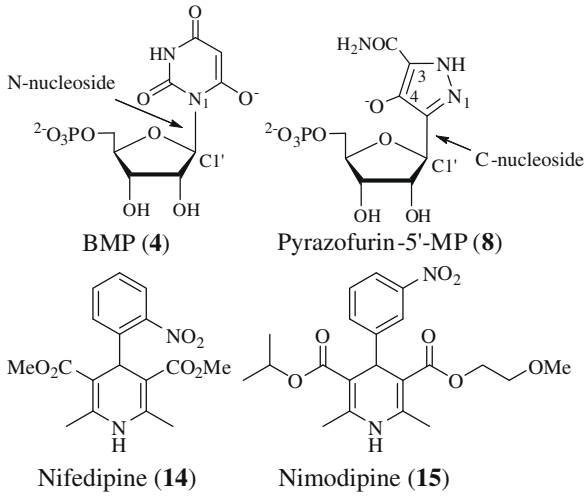

Figure 4. Structures of nucleoside and non-nucleoside inhibitors of ODCase.

Compounds **8** and **10** were also evaluated for their potential to inhibit ODCases from *P. falciparum*, *H. pylori*, *M. thermoautotrophicum*, *H. sapiens* and *S. aureus* (Fig. 6 and Table 2). The 5-cyanouridine derivative **10** inhibited *Pf*, *Hp* and *Sa* ODCases with very weak inhibition constants (K_i) of 0.91 ± 0.03, 0.29 ± 0.01 and 0.55 ± 0.007 M, respectively, similar to its inhibition of *Hs* and *Mt* ODCases (K_i = 0.14 ± 0.06 and 0.70 ± 0.02 M, respectively). These poor inhibitory properties also reflect the weak molecular interactions between the 5-cyanouridine derivative **10** and ODCase (Fig. 3B). On the other hand, compound **8** inhibited *Hs*- and *Mt* ODCases following two distinct mechanisms. While it is a competitive inhibitor for *Mt* ODCase with a K_i of 6.2 ± 0.6 μM, it interacts with *Hs* ODCase with a kinetics profile akin to that of a slow, tight binding inhibitor (Table 2). For *Hs* ODCase, the inhibition constant K_i was estimated at 17 nM, about three orders of magnitude better than the one for *Mt* ODCase, but similar to that found for yeast ODCase (Table 2).[35]

Enzyme inhibition patterns and inhibition constants coupled to the structural interactions of **4** and **8** with ODCase imply that these

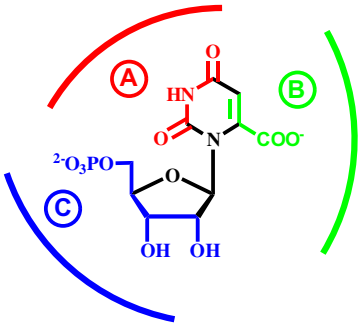

Figure 5. Empirical structure of a proposed pharmacophore for the ligands in the active site of ODCase.

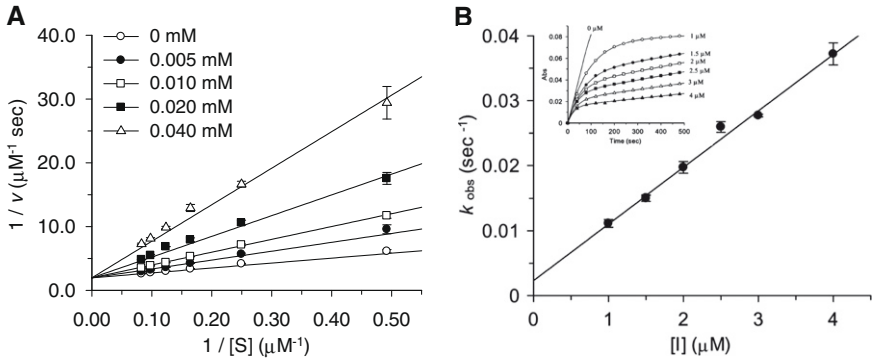

Figure 6. Lineweaver-Burk reciprocal plots to determine the reversible inhibition constant K_i for **8** with *Mt* ODCase (panel A). Panel B depicts the plot of k_{obs} as a function of [**8**] with *Hs* ODCase, and the inset in this panel shows the progress curves of the ODCase reaction in the presence of various concentrations of **8**.

Table 2
Inhibition kinetics for compounds **4**, **8**, and **10** against *Hs*-, *Mt*-, *Pf*-, *Hp*-, *Sa*-, and *Sc*ODCases

Enzyme	K_i (mM)		
	4	**8**	**10**
Hs ODCase	—	1.7×10^{-5}	—
Mt ODCase	—	$6.2 \pm 0.6 \times 10^{-3}$	—
Pf ODCase	—	—	$9.1 \pm 0.3 \times 10^{2}$
Hp ODCase	—	$1.3 \pm 0.6 \times 10^{-4}$	$2.9 \pm 0.1 \times 10^{2}$
Sa ODCase	—	—	$5.5 \pm 0.07 \times 10^{2}$
Sc ODCase[35]	9×10^{-9}	5×10^{-6}	—

compounds are close mimics of the presumed transition-state of the decarboxylation reaction catalyzed by ODCase.[1] It is highly probable that deviations from these molecular structures when designing new inhibitors would compromise the binding affinities towards ODCase. This should, however, not be viewed as a negative feature because tighter binding to the enzyme does not necessarily imply higher potency at the cellular level or a better in vivo efficacy. These latter features are virtues due to physicochemical and biopharmaceutical properties associated with individual inhibitors. This is clearly evident in this set of compounds; despite its three orders of magnitude weaker affinity when compared to **4**, compound **8** nevertheless exhibited good therapeutic potential, which led to the evaluation of compound **7** in phase I clinical trials.[56,12]

Dissection of the ODCase ligand structure. Using the information from the above complexes, and several other three-dimensional structures of ODCases with nucleotide inhibitors, an empirical dissection of the ligand structure is presented in Figure 5. There are three critical regions in the binding site, to which these inhibitors appeal to, especially the nucleoside derivatives. Region A (highlighted in red) may be important in properly orienting the nucleic base moiety. The size and electronic characteristics of the substitutions in region B (in green, Fig. 5) will influence potency and the overall inhibitory characteristics of the ligand. For example, iodo- and azido-substitutions replacing the carboxyl moiety in OMP (**1**) result in formation of a covalent bond to a lysine residue, and a nitrile moiety at the C6 position of UMP (**2**) is catalytically converted into BMP (**4**), a very potent inhibitor of ODCase.[23,27,26] As seen in the co-crystal structure of compound **10** and *Hs* ODCase, the 5-cyano group on the ligand closely fills a hydrophobic pocket, as was also seen with other 5-substitutions such as in 5-fluoro-UMP.[25,57] Interestingly, the presence of a 5-fluoro moiety when combined with a 6-amido group (data not shown here) did not favor the inhibition of ODCase but produced one of the least potent compounds thus far.[23,26,28] It is also interesting to note that ODCase exhibits structural plasticity in its interactions with the C5 and C6 positions of region B of the pyrimidine moiety.[25,28] One thus could incorporate a variety of small to medium size substitutions in region B of the ligand.

The third region, region C (in blue, Fig. 5), especially the 5′-monophosphate moiety, is responsible for maintaining the tight binding of the inhibitor to the active site and defines the minimal characteristics essential for effective binding to this active site and directing the rest of the ligand into the binding site of ODCase. The importance of the monophosphate moiety for ligand binding has been eloquently discussed by others and its contributions towards the binding energy estimated to be as high as 11 kcal/mol.[1] Such large contributions from a remote and non-reacting phosphoryl group also play an important role for catalysis in other enzymes, for example, triose phosphate isomerase, and such an effect is not unique to ODCase.[58] Thus anionic charges located in region C on the ligand, either due to a phosphate moiety or other anionic groups as part of unrelated structural features, possibly discovered through lead hopping, should convey high affinity to potential inhibitors. This will provide an opportunity for novel inhibitor design, with the potential of steering the core structure away from 'nucleoside'-like compounds.

Interestingly, as briefly mentioned above, two widely prescribed calcium channel blockers, nifedipine and nimodipine are also moderately potent inhibitors of ODCase with K_i values of 105 and 18 μM, respectively.[53] It is quite intriguing to discover that non-nucleoside compounds can compete for the same binding site on ODCase as the natural nucleotide substrate(s). Our experiments to obtain crystals of ODCase complexes of the channel blockers did not succeed, thus we conducted comprehensive computational docking experiments to better understand how these non-nucleosides might bind in the active site of ODCase (Fig. 7). Both compounds fit well into the active site of ODCase, and interestingly the nitro moiety on the phenyl group interacts with the cationic Arg262 (this residue also anchors the monophosphate group in nucleotide ligands which is a major contributor to the ligands' binding energy). The two cyclic moieties in both nifedipine (**14**) and nimodipine (**15**) span the interior of the active site, an area with which nucleoside substrates typically do not interact. The side chains, methoxycarbonyl and methoxyethoxycarbonyl moieties on the dihydropyridine of **14** and **15**, respectively, bind at the hydrophobic site where C-5 substitutions of nucleoside ligands interact. The carbonyl moiety on these side chains interacts with Gln241 and Gly229. These docked models reinforce the idea that one can achieve ODCase inhibition via structural features other than those of nucleosides.

In order to ascertain the conformational preferences and the binding mode of nucleotide analogs, we undertook an analysis of co-crystal structures of eleven inhibitors bound in the active site

of ODCase (Fig. 8). Briefly, the bound ligands were extracted from the active site of ODCase and were overlapped at three atoms: N1, C1′ and C4′ in order to compare their bound conformations. Predominately these molecules assumed 2′-endo/3′-exo conformation and indicated little influence onto the proposed pharmacophore model (Fig. 5). We note here that there are exceptions to this generality, and we revealed through a comprehensive analysis that nucleotides such as CMP and XMP assume diverse conformations.[28] Currently there is little experimental and/or theoretical evidence to draw conclusions on the unbound conformations of the nucleotides and their binding preferences to ODCase, which are also the limitations of the current study.

The generic pharmacophore proposed in Figure 5 although was based on nucleotide ligands, above described two non-nucleosides do indeed follow the regions B and C for their interactions with ODCase. Therefore, the dissection of the structural determinants for the binding of ligands to ODCase presented here will aid in the design of novel nucleoside as well as non-nucleoside inhibitors. In summary, we present a comprehensive analysis of structurally diverse ligands against ODCase generating an empirical set of principles for ligand interactions. These principles are applicable for the design of new generation of inhibitors targeting ODCase.

Figure 8. Overlap of eleven ligands bound in the active site of ODCase, obtained from the corresponding co-crystal structures. All inhibitors are shown in capped-stick representation: blue: UMP, cyan: 6-aza-UMP, green: 5-I-UMP, greenblue: BMP, magenta: 6-NH2-UMP, orange: 5-Br-UMP, purple: 5-CN-UMP, red: OMP, red–orange: 5-F-UMP, violet: 6-acetyl-UMP, yellow: 6-I-UMP.

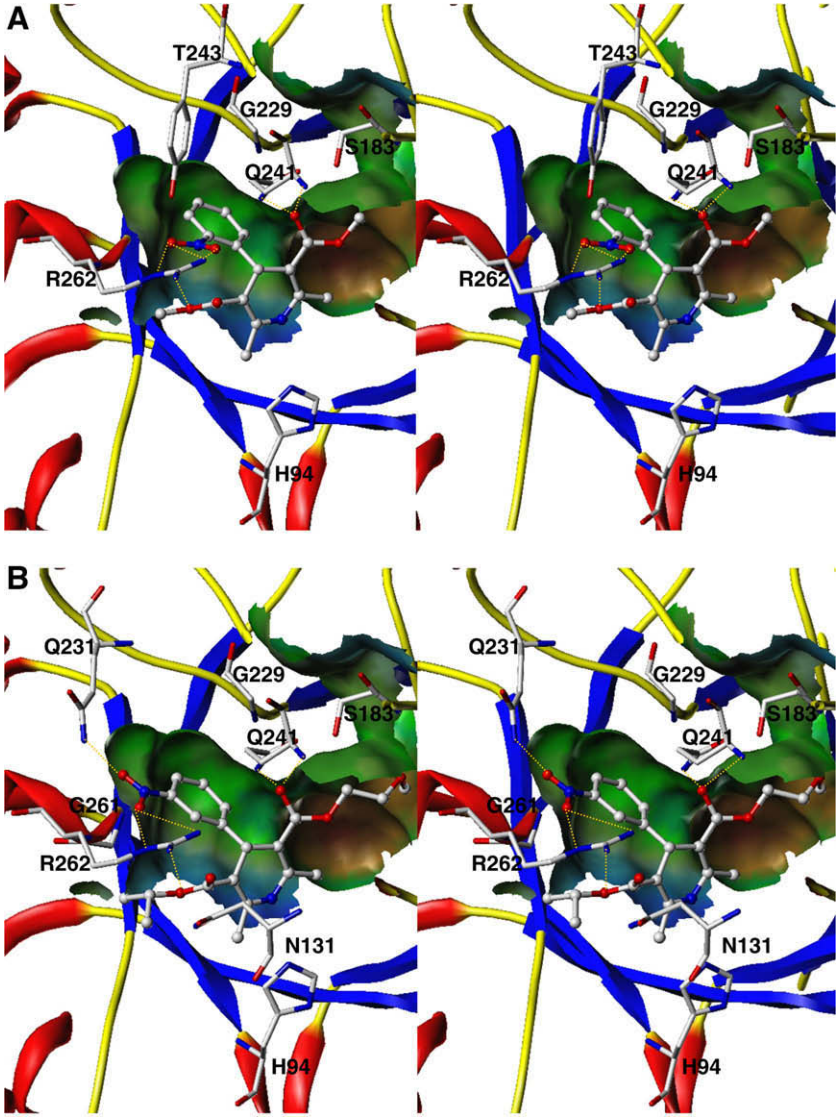

Figure 7. Stereo view of the active site of *Hs* ODCase with docked nifedipine (panel A) and nimodipine (panel B). The ligand is shown in a ball-and-stick representation and the residues of the enzyme are displayed by a capped-tick model; atoms are color-coded according to atom type. The backbone of the enzyme is rendered according to secondary structure, and a portion of the active site is rendered using a Connolly surface with lipophilic character. A potential hydrogen-bonding network is shown by dashed lines in orange.

Acknowledgments

The authors thank Mr. Terence To for help with the expression and purification of ODCase enzymes and Professor David Clarke for generously allowing the use of the ITC instrument. This work was supported by grants from the Canadian Institutes of Health Research (EFP & LPK) and by the University of North Carolina at Greensboro (LPK). E.F.P. acknowledges support through the Canada Research Chairs program. We thank the staff at BioCARS, sector 14 beamlines at the Advanced Photon Source, Argonne National Laboratories, for their generous time commitments and support. Use of the Advanced Photon Source was supported by the Basic Energy Sciences, Office of Science, United States Department of Energy, under Contract W-31-109-Eng-38. Use of the BioCARS sector 14 was supported by the National Center for Research Resources, National Institutes of Health, under Grant RR07707. We also gratefully acknowledge the help we received from the staff of the Canadian Macromolecular Crystallography Facility, at the Canadian Light Source, which is supported by NSERC, NRC, CIHR, and the University of Saskatchewan.

References and notes

1. Miller, B. G.; Wolfenden, R. *Ann. Rev. Biochem.* **2002**, *71*, 847.
2. Miller, B. G. *Top. Curr. Chem.* **2004**, *238*, 43.
3. Ning, W.; Pai, E. F. *Top. Curr. Chem.* **2004**, *238*, 23.
4. Jones, M. E. *Annu. Rev. Biochem.* **1980**, *49*, 253.
5. Reyes, P.; Guganig, M. E. *J. Biol. Chem.* **1975**, *250*, 5097.
6. McClard, R. W.; Black, M. J.; Livingstone, L. R.; Jones, M. E. *Biochemistry* **1980**, *19*, 4699.
7. Reichard, P. *Adv. Enzymol. Mol. Biol.* **1959**, *21*, 263.
8. Donovan, W. P.; Kushnerm, S. R. *J. Bacteriol.* **1983**, *156*, 620.
9. Pragobpol, S.; Gero, A. M.; Lee, C. S.; O'Sullivan, W. J. *Arch. Biochem. Biophys.* **1984**, *230*, 285.
10. Krungkrai, S. R.; Prapunwattana, P.; Horii, T.; Krungkrai, J. *Biochem. Biophys. Res. Commun.* **2004**, *318*, 1012.
11. Gero, A. M.; O'Sullivan, W. J. *Blood Cells* **1990**, *16*, 467.
12. Christopherson, R. I.; Lyons, S. D.; Wilson, P. K. *Acc. Chem. Res.* **2002**, *35*, 961.
13. Seymour, K. K.; Lyons, S. D.; Phillips, L.; Rieckmann, K. H.; Christopherson, R. I. *Biochemistry* **1994**, *33*, 5268.
14. Krungkrai, J.; Krungkrai, S. R.; Phakanont, K. *Biochem. Pharmacol.* **1992**, *43*, 1295.
15. Smiley, J. A.; Saleh, L. *Bioorg. Chem.* **1999**, *27*, 297.
16. Gabrielsen, B.; Kirsi, J. J.; Kwong, C. D., et al *Antiviral Chem. Chemother.* **1994**, *5*, 209.
17. Nord, L. D.; Willis, R. C.; Smee, D. F.; Riley, T. A.; Revankar, G. R.; Robins, R. K. *Biochem. Pharmacol.* **1988**, *37*, 4697.
18. Smee, D. F.; McKernan, P. A.; Nord, L. D.; Willis, R. C.; Petrie, C. R.; Riley, T. M.; Revankar, G. R.; Robins, R. K.; Smith, R. A. *Antimicrob. Agents. Chemother.* **1987**, *31*, 1535.
19. Morrey, J. D.; Smee, D. F.; Sidwell, R. W.; Tseng, C. *Antiviral Res.* **2002**, *55*, 107.
20. Toth, K.; Amyes, T. L.; Wood, B. M.; Chan, K.; Gerlt, J. A.; Richard, J. P. *J. Am. Chem. Soc.* **2007**, *129*, 12946.
21. Van Vleet, J. L.; Reinhardt, L. A.; Miller, B. G.; Sievers, A.; Cleland, W. W. *Biochemistry* **2008**, *47*, 798.
22. Wu, N.; Mo, Y.; Gao, J.; Pai, E. F. *Proc. Natl. Acad. Sci. U.S.A.* **2000**, *97*, 2017.
23. Lee, J. K.; Tantillo, D. J. *Adv. Phys. Org. Chem.* **2003**, *38*, 183.
24. Wepukhulu, W. O.; Smiley, V. L.; Vemulapalli, B.; Smiley, J. A.; Phillips, L. M.; Lee, J. K. *Org. Biomol. Chem.* **2008**, *6*, 4533.
25. Fujihashi, M.; Bello, A. M.; Poduch, E.; Wei, L.; Annedi, S. C.; Pai, E. F.; Kotra, L. P. *J. Am. Chem. Soc.* **2005**, *127*, 15048.
26. Fujihashi, M.; Bello, A. M.; Kotra, L. P.; Pai, E. F. *J. Mol. Biol.* **2009**, *387*, 1199.
27. Wittmann, J. G.; Heinrich, D.; Gasow, K.; Frey, A.; Diederchisen, U.; Rudolph, M. G. *Structure* **2008**, *16*, 82.
28. Poduch, E.; Wei, L.; Pai, E. F.; Kotra, L. P. *J. Med. Chem.* **2008**, *51*, 432.
29. Bello, A. M.; Poduch, E.; Fujihashi, M.; Amani, M.; Li, Y.; Crandall, I.; Hui, R.; Lee, P. I.; Kain, K. C.; Pai, E. F.; Kotra, L. P. *J. Med. Chem.* **2007**, *50*(5), 915.
30. Bello, A. M.; Poduch, E.; Liu, Y.; Wei, L.; Crandall, I.; Wang, X.; Dyanand, C.; Kain, K. C.; Pai, E. F.; Kotra, L. P. *J. Med. Chem.* **2008**, *51*, 439.
31. Meza-Avina, M. E.; Wei, L.; Buhendwa, M. G.; Poduch, E.; Bello, A. M.; Pai, E. F.; Kotra, L. P. *Mini-Rev. Med. Chem.* **2008**, *8*, 239.
32. De Clercq, E. *Future Virol.* **2006**, *1*, 19.
33. Van Rompay, A. R.; Johansson, M.; Karlsson, A. *Pharmacol. Ther.* **2003**, *100*, 119.
34. Williams, R. H.; Hoehn, M. M. US Patent# 3,674,774, 1972.
35. Williams, R. H.; Gerzon, K.; Hoehn, M.; Gorman, M.; DeLong, D. C. Abstract# MICR 38, 158th American Chemical Society National Meeting, New York, NY, 1969.
36. Dix, D. E.; Lehman, C. P.; Jakubowski, A.; Moyer, J. D.; Handschumacher, R. E. *Cancer Res.* **1979**, *39*, 4485.
37. Cadman, E.; Eiferman, F.; Heimer, R.; Davis, L. *Cancer Res.* **1978**, 4610.
38. Matsumoto, S. S.; Fujitaki, J. M.; Dee Nord, L.; Willis, R. C.; Lee, V. M.; Sharma, B. M.; Sanghvi, Y. S.; Kini, G. D.; Revankar, G. R.; Robins, R. K.; Jolley, W. B.; Smith, R. A. *Biochem. Pharmacol.* **1990**, *39*, 455.
39. Gutowski, G. E.; Sweeney, M. J.; DeLong, D. C.; Hamill, R. L.; Gerzon, K. *Ann. N.Y. Acad. Sci.* **1975**, *255*, 544.
40. Andrei, G.; De Clercq, E. *Antiviral Res.* **1993**, *22*, 45.
41. Wyde, P. R.; Gilbert, B. E.; Ambrose, M. W. *Antiviral Res.* **1989**, *11*, 15.
42. De Clercq, E. *Clin. Microbiol. Rev.* **2001**, 382.
43. Scott, H. V.; Gero, A. M.; O'Sullivan, W. J. *Mol. Biochem. Parasitol.* **1986**, *18*, 3.
44. Elgemeie, G. H.; Zaghary, W. A.; Amin, K. M.; Nasr, T. M. *Nucleosides Nucleotides Nucleic Acids* **2005**, *24*, 1227.
45. Golemi-Kotra, D.; Pai, E. F.; Kotra, L. P., unpublished results.
46. Poduch, E.; Bello, A. M.; Tang, S.; Fujihashi, M.; Pai, E. F.; Kotra, L. P. *J. Med. Chem.* **2006**, *49*, 4937.
47. Otwinowski, Z.; Minor, W. *Methods Enzymol.* **1997**, *276*, 307.
48. Vagin, A.; Teplyakov, A. *J. Appl. Cryst.* **1997**, *30*, 1022.
49. Murshudov, G. N.; Vagin, A. A.; Dodson, E. J. *Acta Crystallogr., Sect. D* **1997**, *53*, 240.
50. Emsley, P.; Cowtan, K. *Acta Crystallogr., Sect. D* **2004**, *60*, 2126.
51. Levine, H. L.; Brody, R. S.; Westheimer, F. H. *Biochemistry* **1980**, *19*, 4993.
52. Otter, B. A.; Falco, E. A.; Fox, J. J. *J. Org. Chem.* **1969**, *34*, 1390.
53. Miller, B. G.; Snider, M. J.; Short, S. A.; Wolfenden, R. *Biochemistry* **2000**, *39*, 8113.
54. Amyes, T. L.; Richard, J. P.; Tait, J. J. *J. Am. Chem. Soc.* **2005**, *127*, 15708.
55. Najarian, T.; Traut, T. W. *Neurorehabil. Neural Repair* **2000**, *14*, 237.
56. Cadman, E. C.; Dix, D. E.; Handschumacher, R. E. *Cancer Res.* **1978**, *38*, 682.
57. Bello, A. M.; Konforte, D.; Poduch, E.; Furlonger, C.; Wei, L.; Liu, Y.; Lewis, M.; Pai, E. F.; Paige, C. J.; Kotra, L. P. *J. Med. Chem.* **2009**, *52*, 1648.
58. Morrow, J. R.; Amyes, T. L.; Richard, J. P. *Acc. Chem. Res.* **2008**, *41*, 539.